INTERNATIONAL SOCIETY FOR
SOIL MECHANICS AND
GEOTECHNICAL ENGINEERING

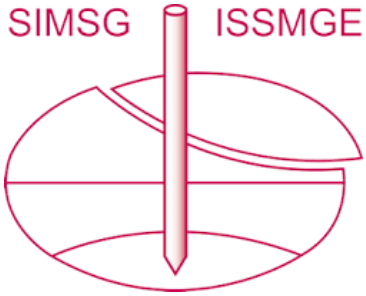

This paper was downloaded from the Online Library of the International Society for Soil Mechanics and Geotechnical Engineering (ISSMGE). The library is available here:

https://www.issmge.org/publications/online-library

This is an open-access database that archives thousands of papers published under the Auspices of the ISSMGE and maintained by the Innovation and Development Committee of ISSMGE.

Thin soil layer detection by VisCPT and FEM simulations

Mince couche de sol et de la détection par VisCPT FEM simulations

R. D. Hryciw & Y. Jung
University of Michigan, USA

E. Susila
Bandung Institute of Technology, Indonesia

A. Ibrahim
Mansoura University, Egypt

ABSTRACT

A comprehensive approach for locating, characterizing the dominant grain size and estimating the strength of thin anomalous layers in a cohesionless soil stratigraphy is presented. The approach utilizes the results of finite element simulations of cone penetration across thin layers of anomalous strength and identification of their location and thickness using the Vision Cone Penetrometer (VisCPT). Through developed image processing algorithms based on wavelet decomposition, the dominant grain size in soil images is obtained. FEM simulations utilizing adaptive remeshing reveal the changes in CPT tip resistance across thin layers. Field data confirms the VisCPT's ability to detect thin layers that are often missed by the conventional CPT.

RÉSUMÉ

Une approche globale de la localisation, la caractérisation de la taille des grains dominante et l'estimation de la force de couches minces anormale dans un sol cohesionless stratigraphie est présenté. L'approche utilise les résultats de simulations par éléments finis de la pénétrabilité au cône à travers des couches minces de force et de l'identification des anomalies de leur emplacement et de l'épaisseur à l'aide du cône Pénétromètre Vision (VisCPT). Grâce à des algorithmes de traitement d'image développé repose sur la décomposition en ondelettes, la dominante la taille des grains dans le sol, les images obtenues. FEM simulations utilisant remaillage adaptatif révèlent les changements dans CPT pointe à travers la résistance des couches minces. Les données de terrain confirme l'VisCPT de la capacité de détecter des couches minces qui sont souvent manqués par l'conventionnel CPT.

Keywords : cone penetration test, vision, grain size, finite element method, in-situ testing, site characterization, image processing

1 INTRODUCTION

The cone penetration test (CPT) is the geotechnical engineering standard for high quality site characterization and in-situ estimation of geomechanical properties. Among its advantages over the standard penetration test (SPT) is the continuous recording of penetration resistance with depth. Its primary disadvantage is that no soil specimen is recovered for visual inspection and laboratory testing. However, even the advantage listed above may be questioned if the soils are highly stratified. Meanwhile, the stated disadvantage now has a partial remedy.

Empirical correlations for soil type based on CPT *tip resistance* (or cone bearing), q_c and CPT *friction ratio* (the ratio of side friction to end bearing) date back several decades (Begemann 1965; Douglas & Olsen 1981; Robertson 1990; Robertson & Campanella 1983; Sanglerat 1972). In general, high tip resistances and low friction ratios indicate coarse-grained soil while low tip resistance and high friction ratios indicate fine-grained material. The tip resistances in sands are commonly used to predict geomechanical soil properties including the effective (drained) angle of shearing resistance, ϕ' (Baldi et al. 1981; Belloti et al. 1982; Durgunoglu & Mitchell 1975a; Durgunoglu & Mitchell 1975b; Ghionna & Jamiolkowski 1991; Houlsby & Hitchman 1988; Janbu & Senneset 1974; Kiousis et al. 1988; Salgado et al. 1997; Salgado & Prezzi 2007; Susila & Hryciw 2003; Van Den Berg et al. 1996; Yu & Mitchell 1998). However, the resistances to cone penetration comes from soil strength mobilized over a depth increments as large as 10 to 15 cone diameters above and below the tip. A smaller influence zone exists for loose contractile sands while a larger zone influences q_c in dense dilatant sand. As a result, if the stratigraphy is thinly bedded, the recorded q_c reflects an averaged response of the layers rather than indicating the strength of any individual layer.

The CPT signature across interfaces between distinct layers was studied to help better locate the interface (Hryciw & Shin 2004). Anomalous and misleading spikes in friction ratio were observed to develop at, just above or just below interfaces, but always in the weaker soil. This was later confirmed by finite element studies (Hryciw et al. 2005).

In the case of single thin anomalous layers, if the thin layer is of low strength but surrounded by stronger sands, the stronger sands would keep the q_c observed through the weak sand from dropping to values reflective of its true lower strength. Conversely, if a thin high strength layer is surrounded by weaker sands, the weaker sands would keep the strong sand from exhibiting its full resistance. In either case, the undeveloped q_c of the thin layer can lead to misclassification of the soil and overestimates or underestimates of strength. In this paper, the word "thin" is used to describe a layer in which q_c can not fully develop as it would if the entire zone of influence were located within the layer. The actual thickness of a so-called "thin" layer will prove to be surprisingly large in some cases.

2 FEM SIMULATIONS WITH ADAPTIVE REMESHING

Finite element studies were performed to quantify the effect of "thin" layers of various thicknesses on the development of q_c as the cone tip approaches a thin layer, passes through and exits. The strengths of the thin layer were varied relative to the strengths of the soil above and below. The ultimate goal is to develop corrections to the observed q_c to estimate the so called "fully developed q_c" from which the soil could be correctly classified and from which fundamental soil properties of the thin layer could be determined.

Proceedings of the 17th International Conference on Soil Mechanics and Geotechnical Engineering
M. Hamza et al. (Eds.)
© 2009 IOS Press.
doi:10.3233/978-1-60750-031-5-1052

The numerical studies required advanced adaptive remeshing tools provided in the commercial FEM software Abaqus to deal with very large soil strains beneath and adjacent to the advancing cone. The dimensions of the simulation and element types are shown in Fig. 1 while the non-linear soil model is detailed by Susila & Hryciw (2003).

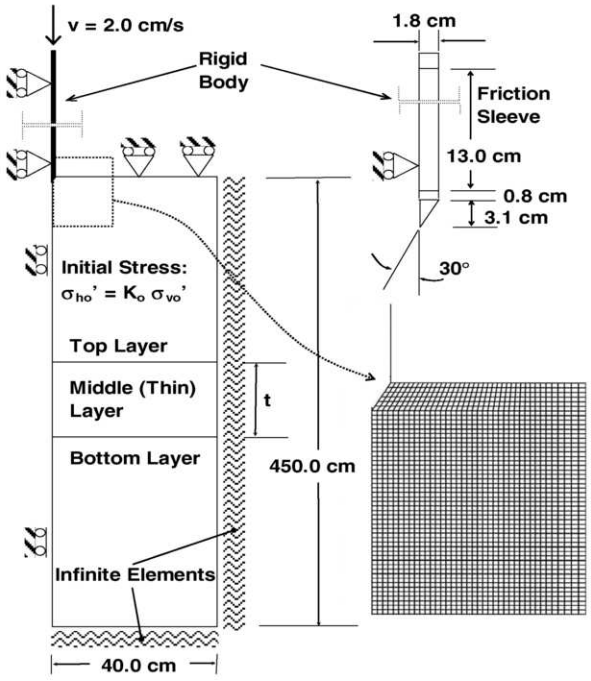

Figure 1. Finite element simulation dimensions and grid (after Susila 2005).

In a parametric study, the angles of internal shearing resistance (ϕ') of both the thin layer and surrounding soil were varied in two degree increments between 32° and 42°. The sand stiffness and angle of dilation for each ϕ' were adjusted using established geomechanical relationships (Susila & Hryciw 2003).

Figures 2 and 3 show typical results from the FEM simulations. In both figures, the zero point on the vertical axis represents the mid-height of a thin layer. The thickness of the thin layer thickness is varied from 2 cm to 100 cm. In Figure 2, a weak thin layer (ϕ'=32°) is bounded on top and bottom by a much stronger (ϕ'=42°) soil. The sequence is reversed in Fig. 3 where a strong thin layer (ϕ'=42°) is bounded on top and bottom by the weaker (ϕ'=32°) soil.

The figures show that when the thickness of the middle layer is less than about 30 cm to 50 cm, the q_c of the middle layer does not develop a steady plateau. For thicknesses of 100 cm, the q_c plateau always develops.

Other results revealed that the larger the ϕ' of the middle layer, the larger is the thickness needed to achieve a q_c plateau. Figures 2 and 3 also show that q_c begins to change well before the cone encounters the thin layer. As could have been expected, the tip resistance drops sooner when the cone penetrometer advances from a higher ϕ' sand towards a lower ϕ' thin layer (Fig. 2) than it rises when the cone penetrometer advances from a lower ϕ' sand towards a higher ϕ' thin layer (Fig. 3).

The results of Figures 2, 3 and similar others of varying ϕ' were used by Susila (2005) to develop correction factors for ϕ' based on the differences in ϕ' between layers and the thin layer thickness. The problem with this approach is that the thin layer thickness must be known to implement the correction. This is addressed in-situ by the Vision Cone Penetrometer (VisCPT) as discussed next.

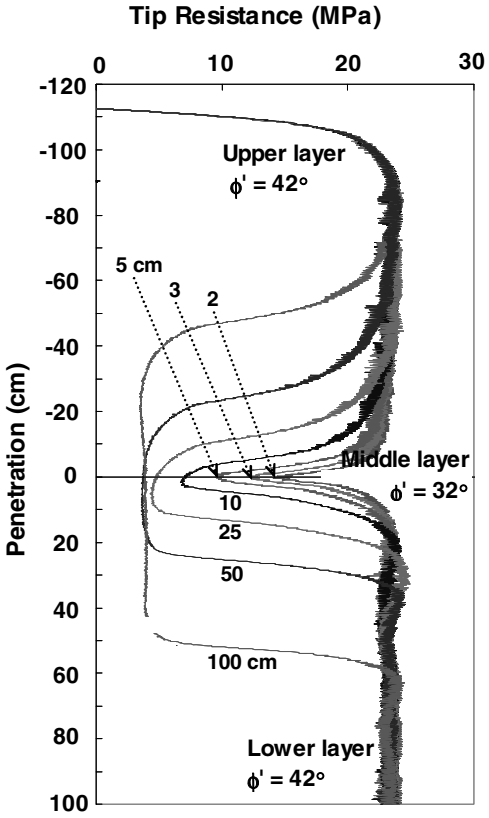

Figure 2. Penetration of a stronger-weaker-stronger sand sequence with the strong middle layer varying in thickness (Susila 2005).

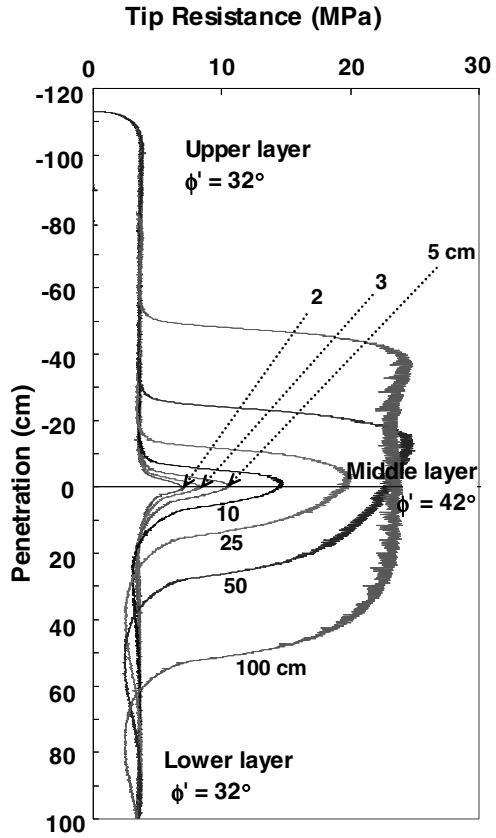

Figure 3. Penetration of a weaker-stronger-weaker sand sequence with the weak middle layer varying in thickness (Susila 2005).

3 VISION CONE PENETROMETER AND IMAGE PROCESSING

The major disadvantage of the conventional CPT; lack of a recovered soil specimen for observation, was partially overcome by development of the Vision Cone Penetrometer (VisCPT) (Jung et al. 2008; Raschke & Hryciw 1997). Shown in Fig. 4, the VisCPT captures continuous soil images by videotaping the soil through a sapphire window.

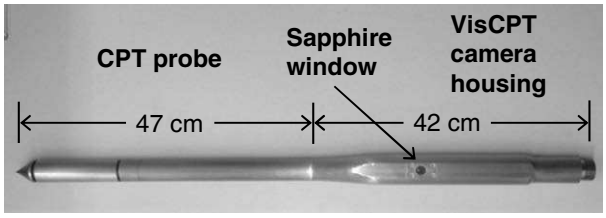

Figure 4. Vision cone penetrometer (VisCPT) for obtaining subsurface soil images.

A wavelet decomposition index (*CA*) was introduced (Shin & Hryciw 2004) for determining soil grain size from 256 pixel x 256 pixel images taken in the laboratory or in-situ by the VisCPT. At a fixed camera magnification, grain sizes over 1.5 orders of magnitude can be determined. For example, all medium and fine sand particles from 2 mm (#10 standard US sieve) to 0.075 mm (#200 sieve) can be correctly identified with a single camera magnification. By varying the camera magnification, the method can be extended to a much wider range of grain sizes, from coarse gravel to very fine silt.

For grain size assessment by digital image processing methods, Hryciw et al. (2006) advocate use of the number of image pixels per grain diameter (*PPD*) instead of the actual grain size. The relationship between *CA* and *PPD* obtained from various soils is shown in Fig. 5. A best-fit model to the data is:

$$\log_{10} PPD = A \log_{10} (CA/CA_1) \quad (1)$$

where CA_1 is the *CA* corresponding to *PPD* = 1.0 and *A* is an empirical constant equal to 5.5 +/- 0.4. The lower limit of $A \approx 5.1$ was observed when soil was saturated and behind glass. Jung et al. (2008) previously found *CA* to be about 0.24 higher at all *PPD*s for the same soil when photographed in a saturated state behind glass than in a dry exposed condition. The present data shown in Figure 5 refines this earlier observation.

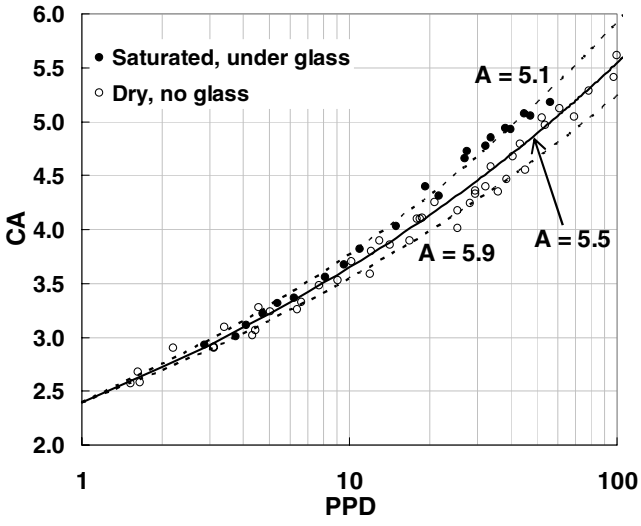

Figure 5. Calibration curves for image processing by wavelets.

A laboratory specimen containing a "thin" soil layer is shown in Fig. 6. It was prepared by sedimenting the soil through water in a long glass tube of 5 cm by 5 cm cross-section. The thin layer in Fig. 6 consists of uniform soil grains retained between a #30 (0.59 mm opening) sieve and a #40 (0.42 mm opening) sieve. The thin layer thickness was 9.3 mm. The overlying and underlying soil is also uniform with grains retained between a #100 (0.149 mm opening) and a #120 (0.125 mm opening) sieve. Fig. 6 also shows the *CA* log obtained by scanning the sedimented soil column (just as by the VisCPT). and image processing overlapping 256 pix. by 256 pix. regions. The white "sampling window" in Fig. 6 shows the size of the 256 pix. x 256 pix. region used for computing each *CA*. The *CA* of the finer soil was approximately 3.0 while the coarser sand showed *CA* = 4.0. Equation (1) with *A*=5.5 yields PPDs of 3.4 for the finer sand and 16.6 for the coarser sand. The camera magnification was 30.4 pix/mm thus the computed grain sizes are 0.11 mm and 0.55 mm respectively. Considering the orders of magnitude range of possible grain sizes, these values should be considered as being in very good agreement with the grain sizes determined by sieving.

Referring once again to Figure 6 the *CA* begins to increase at a depth of 2.68 cm and returns to the background (fine soil) *CA* value at 4.44 cm for a total excursion interval of 1.76 cm. With camera magnification at 30.4 pixels/mm this interval is 534 pixel units. For 256 pixel x 256 pixel images the thickness of the "thin" layer will always be equal to the excursion interval (in pixels) minus 256 pixels. Thus, the thin layer is detected to be 278 pixels or 9.1 mm width.

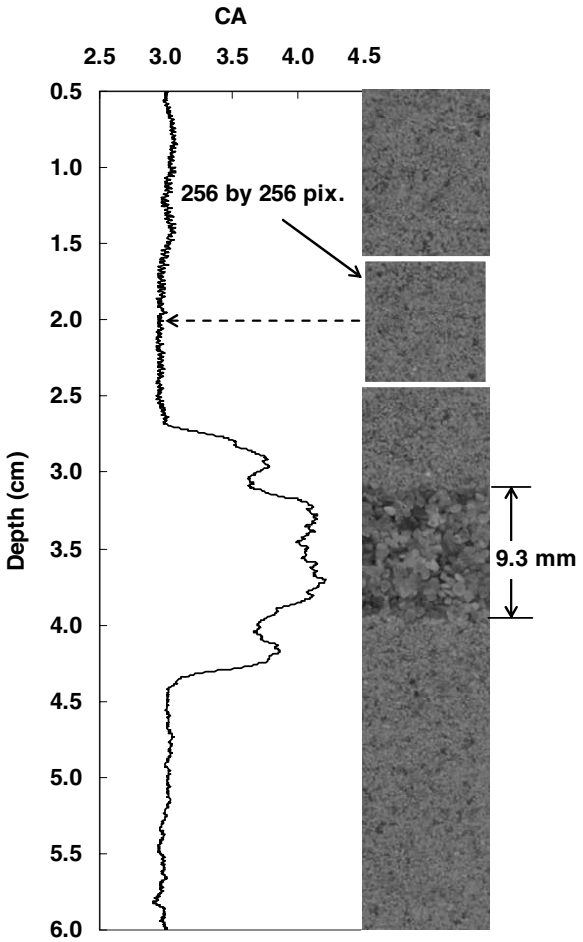

Figure 6. Wavelet Index (*CA*) for a thin lens of coarser sand with finer sand above and below.

4. THIN LAYER DETECTION BY VisCPT

Vision cone penetrometer data was collected at three sites in the states of Indiana and Kansas in the United States. The electronic CPT data sampling interval was 2 cm. Thin layers of either lower or higher q_c than the surrounding soil were observed at all three sites. In all cases the change in q_c was due to a change in soil grain size significant enough to register as a change in "soil type" according to Robertson (1990). A comparison is made between the thickness of the "thin" layers as predicted by the CPT test and as observed by the VisCPT in Figure 7. In most cases the CPT underpredicted the actual thickness by several centimeters. When the "thin" layer was 10 cm or less the CPT occasionally missed the layer altogether.

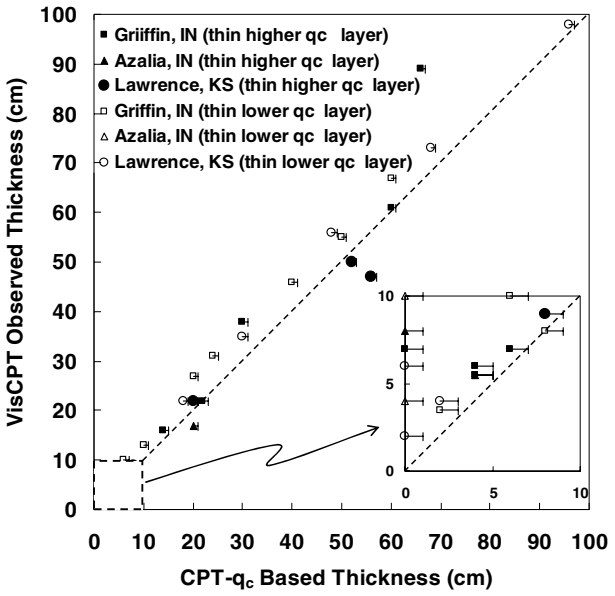

Figure 7. Comparison of thin layer thicknesses predicted by the CPT and as observed by the VisCPT.

5 CONCLUSIONS

The combination of FEM modeling utilizing autoadaptive remeshing and in-situ soil observation by the Vision Cone Penetrometer (VisCPT) provides a powerful solution to thin layer delineation and characterization. Neither tool alone can characterize the soil in terms of both the mechanical properties and vertical distribution by soil type. Through wavelet decomposition of images, the soil grain size and the thicknesses of "thin" layers are determined. In-Situ VisCPT testing revealed that the conventional CPT slightly underpredicts layer thicknesses and occasionally misses them altogether when their thickness is less than 10 cm.

ACKNOWLEDGEMENTS

Funding for this study was partially provided by the US National Science Foundation's Civil, Mechanical and Manufacturing Innovations Division, Geomechanics and Geotechnical Systems Program Grant #0324444. Any opinions, findings, conclusions or recommendations expressed in this paper are those of the authors and do not necessarily reflect the views of the National Science Foundation.

REFERENCES

Baldi, G., Bellotti, R., Ghionna, V., Jamiolkowski, M., & Pasqualini. 1981. Cone resistance of a dry medium sand, Proc. of the 10th Int. Conf. on Soil Mech. and Foundation Eng., Stockholm, 2: 427-432.

Begemann, H.K. 1965. The friction jacket cone as an aid in determining the soil profile, Proc. of the 6th Int. Conf. on Soil Mechanics and Foundation Eng., 1: 17-20.

Belloti, R., Bizzi, G., & Ghionna. V. 1982. Design, construction, and use of a calibration chamber, Proc., ESOPT II. Balkema, Amsterdam, The Netherlands, 2: 439-446.

Douglas, B.J. & Olsen, R.S. 1981. Soil classification using electric cone Penetrometer, Symp. on Cone Penetration Testing and Experience, Geotechnical Eng. Div. of ASCE, St.Louis, MO, 209-227.

Durgunoglu, H. T. & Mitchell, J. K. 1975a. Static penetration resistance of soils: I. Analysis. Proc. of the Conf. on In Situ Measurement of Soil Properties, ASCE, New York, NY, 1: 151-171.

Durgunoglu, H.T. & Mitchell, J. K. 1975b. Static penetration resistance of soils: II. Evaluation of theory and implications for practice, Proc. of the Conf. on In Situ Measurement of Soil Properties, ASCE, New York, NY, 1: 172-189.

Ghionna, V. & Jamiolkowski, M. 1991. A critical appraisal of calibration chamber testing of sands, Proc. of the 1st Int. Symp. on Calibration Chamber Testing (ISOCCT1), A. B. Huang, ed. Elsevier Applied Science, New York, NY: 13-39.

Houlsby, G. T. & Hitchman, R. 1988. Calibration Chamber Tests of a Cone Penetrometer in Sand. *Geotechnique*, 38(1): 39-44.

Hryciw, R.D. & Shin, S. 2004. Thin layer and interface characterization by VisCPT. Proc. of the 2nd Int. Conf. on Site Characterization, Porto, Portugal: 701-706.

Hryciw, R. D., Susila E. & Shin, S. 2005. CPT readings, VisCPT observation, and advanced FEM modeling of penetration through soil interfaces, Proc. of GeoFrontiers 2005, ASCE GSP #138.

Hryciw, R. D., Shin, S. & Jung, Y. 2006. Soil image processing – single grains to particle assemblies, Proc. of Geotechnical Eng. In the Information Technology Age, GeoCongress: 6 pp.

Janbu, N. & Senneset, K. 1974. Effective stress interpretation of in-situ static cone penetration tests. Proc. of the 1st Eur. Symp. On Penetration Testing, 2: 181-193.

Jung, Y., Hryciw, R. D. & Elsworth, D. 2008. Vision cone penetrometer calibration for soil grain size. Proc. of the 3rd Int. Conf. on Site Characterization, Taipei, Taiwan: 1303-1308.

Kiousis, P.D., Voyiadjis, G. Z. & Tumay, M.T. 1988. A large strain theory and its application in the analysis of the cone penetration mechanism, *Int. Jour. for Numerical and Analytical Methods in Geomechanics*, 12: 45-60.

Raschke, S.A. & Hryciw, R. D. 1997. Vision cone penetrometer (VisCPT) for direct subsurface soil observation, ASCE *Jour. of Geotechnical and Geoenvironmental. Eng.*, 123(11): 1074-1076.

Robertson, P.K. & Campanella, R. G. 1983. Interpretation of cone penetration tests – Part I (Sand), *Canadian Geotechnical Jour*., 20(4): 718-733.

Robertson, P.K. 1990. Soil classification using the cone penetration test. *Canadian Geotechnical Jour.*, 27(1): 151-158.

Salgado, R., Mitchell, J.K., & Jamiolkowski, M. 1997. Cavity expansion and penetration resistance in sand. ASCE *Jour. of Geotechnical and Geoenvironmental Eng.*, 123(4): 344-354.

Salgado, R. & Prezzi, M. 2007. Computation of cavity expansion pressure and penetration resistance in sands. *Int. Jour. of Geomechanics*, ASCE, 7(4): 251-265.

Sanglerat, G. 1972. *The Penetrometer and Soil Exploration*. Developments in Geotechnical Engineering, 1, Elsevier Publishing Company, Amsterdam, 464 pp.

Shin S. & Hryciw R.D. 2004. Application of wavelet analysis to soil mass images for particle size determination. ASCE *Jour. of Computing in Civil Eng.*, 18(1): 19-27.

Susila, E. & Hryciw, R.D. 2003. Large displacement FEM modeling of the cone penetration test (CPT) in normally consolidated sand. *Int. Jour. for Numerical and Analytical Methods in Geomechanics*, 27(7): 585-602.

Susila, E. 2005. *Finite element simulation of the cone penetration test in uniform and stratified sand,* a dissertation submitted in partial fulfillment of the requirements for the degree of Doctor of Philosophy, the Univ. of Michigan: 137.

Van Den Berg, P., De Borst, R., & Huetink H. 1996. An Eulerean finite element model for penetration in layered soil, *Int. Jour. for Numerical and Analytical Methods in Geomech.*, 20(12): 865-886.

Yu, H. S. & Mitchell, J.K. 1998. Analysis of cone resistance: review of methods. ASCE *Jour. of Geotechnical and Geoenvironmental Eng.* 124(2): 140-149.